

1  
2  
3  
4 Article type : Research Article (FSB2)  
5  
6

7 **Gene expression profiles of diabetic kidney disease and neuropathy in *eNOS* knockout**  
8 **mice:**  
9 **predictors of pathology and RAS blockade effects**  
10

11 Stephanie A. Eid<sup>2,\*</sup>, Lucy M. Hinder<sup>2,\*</sup>, Hongyu Zhang<sup>1,\*</sup>, Ridvan Eksi<sup>4</sup>, Viji Nair<sup>1</sup>, Sean Eddy<sup>1</sup>,  
12 Felix Eichinger<sup>1</sup>, Meeyoung Park<sup>2</sup>, Jharna Saha<sup>1</sup>, Celine C. Berthier<sup>1</sup>, Hosagrahar V. Jagadish<sup>4</sup>,  
13 Yuanfang Guan<sup>4</sup>, Subramaniam Pennathur<sup>1,3</sup>, Junguk Hur<sup>5</sup>, Matthias Kretzler<sup>1,4</sup>, Eva L.  
14 Feldman<sup>2,#</sup>, Frank C. Brosius<sup>1,3,6,#</sup>  
15

16 Departments of Internal Medicine<sup>1</sup>, Neurology<sup>2</sup>, Molecular and Integrative Physiology<sup>3</sup>, and  
17 Computational Medicine and Biology<sup>4</sup>, University of Michigan Medical School, Department of  
18 Biomedical Sciences, University of North Dakota<sup>5</sup>, and Department of Medicine, University of  
19 Arizona<sup>6</sup>  
20

21  
22 Address for correspondence:

23 Eva L. Feldman, MD, PhD

24 5017 AATBSRB, 109 Zina Pitcher Place, Ann Arbor, MI 48109, U.S.A.

25 Phone: (734) 763-7274; Fax: (734) 763-7275; email: [efeldman@umich.edu](mailto:efeldman@umich.edu)  
26

27 **Running title:** Renal and nerve transcriptomics in *eNOS* KO mice  
28  
29

This is the author manuscript accepted for publication and has undergone full peer review but has not been through the copyediting, typesetting, pagination and proofreading process, which may lead to differences between this version and the [Version of Record](#). Please cite this article as [doi: 10.1002/FSB2.21467](https://doi.org/10.1002/FSB2.21467)

This article is protected by copyright. All rights reserved

30  
31  
32  
33  
34  
35  
36  
37  
38  
39  
40  
41  
42  
43  
44  
45  
46  
47  
48  
49  
50  
51  
52  
53  
54  
55  
56

**Nonstandard Abbreviations**

**DEG:** Differentially expressed gene

**DKD:** Diabetic kidney disease

**DPN:** Diabetic peripheral neuropathy

**eNOS:** Endothelial nitric oxide synthase

**RAS:** Renin-angiotensin-aldosterone system

**SOM:** Self-organizing map

**Abstract**

Diabetic kidney disease (DKD) and diabetic peripheral neuropathy (DPN) are two common diabetic complications. However, their pathogenesis remains elusive and current therapies are only modestly effective. We evaluated genome-wide expression to identify pathways involved in DKD and DPN progression in *db/db eNOS* <sup>-/-</sup> mice receiving renin-angiotensin-aldosterone system (RAS) blocking drugs to mimic the current standard of care for DKD patients. Diabetes and *eNOS* deletion worsened DKD, which improved with RAS treatment. Diabetes also induced DPN, which was not affected by *eNOS* deletion or RAS blockade. Given the multiple factors affecting DKD and the graded differences in disease severity across mouse groups, an automatic data-analysis method, SOM or self-organizing map was used to elucidate glomerular transcriptional changes associated with DKD, whereas pairwise bioinformatics analysis was used for DPN. These analyses revealed that enhanced gene expression in several pro-inflammatory networks and reduced

---

<sup>1</sup> \*S.A.E., L.M.H., and H.Z. should be considered joint first author  
#E.L.F. and F.C.B. should be considered joint senior author

57 expression of development genes correlated with worsening DKD. Although RAS treatment  
58 ameliorated the nephropathy phenotype, it did not alter the more abnormal gene expression  
59 changes in kidney. Moreover, RAS exacerbated expression of genes related to inflammation and  
60 oxidant generation in peripheral nerves. The graded increase in inflammatory gene expression and  
61 decrease in development gene expression with DKD progression underline the potentially  
62 important role of these pathways in DKD pathogenesis. Since RAS blockers worsened this gene  
63 expression pattern in both DKD and DPN, it may partly explain the inadequate therapeutic efficacy  
64 of such blockers.

65

## 66 **Key Words**

67 Diabetic kidney disease, diabetic peripheral neuropathy, RAS blockade, genome-wide expression,  
68 self-organizing map

69

## 70 **Introduction**

71 Diabetic kidney disease (DKD) is the most common cause of end-stage renal disease in the U.S.  
72 (1). It affects 30-40% of all diabetic patients and continues to rise in prevalence in light of the  
73 current diabetic epidemic, particularly of type 2 diabetes (1). Although glycemic regulation as well  
74 as blood pressure control, through pharmacologic inhibition of the renin-angiotensin-aldosterone  
75 system (RAS), produce salutatory effects, there are no therapies to reliably prevent DKD  
76 progression (2). Diabetic peripheral neuropathy (DPN) is even more prevalent than DKD and often  
77 leads to the loss of all sensory modalities in the extremities (3, 4). DPN is responsible for over  
78 60% of non-traumatic lower-limb amputations in the U.S. (3, 4) and managing DPN accounts for  
79 over 27% of the total cost of diabetes treatment (5). Similar to DKD, there are no effective  
80 therapies that slow or reverse DPN, which tends to inexorably progress despite optimal medical  
81 management.

82 One reason for the slow progress in developing adequate therapies is our lack of  
83 understanding of the mechanisms implicated in DKD and DPN pathogenesis. Unraveling  
84 underlying mechanisms is complicated by the likelihood that numerous interrelated molecular  
85 processes cause cellular- and tissue-specific damage as disease progresses (6, 7). Another  
86 challenge is that available therapies targeting a specific mechanism may reduce end-organ damage

87 in one complication but concurrently exacerbate another (8, 9). Thus, comprehensive and unbiased  
88 studies are needed to understand the complex pathogenesis of each complication, with the goal of  
89 developing mechanism-based therapies.

90 Diabetes mouse models that adequately reproduce the human condition are required to  
91 improve our understanding of pathogenic pathways in DKD and DPN and to support pre-clinical  
92 and clinical studies for evaluating available and novel therapeutic strategies (10-12). Moreover,  
93 mouse strains that develop more than one microvascular complication are important for studying  
94 treatment responsiveness across complication-prone tissues, especially because strains like the  
95 C57BL/6J, are resistant to DKD (10). With regards to DPN, we have recently shown in a strain  
96 comparison study that both the C57BLKS and the C57BL/6J as background strains are susceptible  
97 to nerve damage in the face of a metabolic insult and thus would serve as robust models of DPN  
98 (13). We thus performed unbiased genome-wide expression analysis of murine kidney and  
99 peripheral nerve tissue. We selected a model, which was predicted to develop a graded spectrum  
100 of DKD phenotype, from normal to highly progressive disease, through *eNOS* deletion, expected  
101 to accelerate DKD through endothelial dysfunction albuminuria and glomerular lesions (14-16),  
102 and RAS blockade, which is expected to partly ameliorate DKD (17). This C57BLKS *db/db eNOS*  
103 *-/-* mouse appears to be one of the models that best represents human DKD (18). As mentioned  
104 above, the C57BLKS *db/db* mouse model closely mimics human DPN (11, 19). Thus, selecting  
105 the C57BLKS *db/db eNOS -/-* mouse would allow us to analyze gene expression along a spectrum  
106 of disease, including wild-type, diabetic, *eNOS -/-* and diabetic *eNOS -/-* animals, with or without  
107 RAS inhibition.

108 Using an automatic unbiased data-analysis method, we found that worsening DKD was  
109 associated with enhanced gene expression in several pro-inflammatory networks and reduced  
110 expression in kidney development, metabolism, and podocyte genes. Although RAS blockers  
111 ameliorated kidney function, they did not alter the more abnormal gene expression changes in  
112 kidney. RAS blockers also worsened expression of genes involved in inflammation and oxidant  
113 generation in peripheral nerves. Together, these results suggest that the inadequacy of RAS  
114 blockade may result from their inability to restore gene expression in DKD and DPN and advocates  
115 for treatments that will interrupt specific inflammatory pathways for each complication.

116

117 **Methods**

118 Animal model.

119 Four genotypes of male mice on a C57BLKS background were evaluated: (i) diabetic *db/db eNOS*  
120 *-/-* mice; (ii) diabetic *db/db eNOS* *+/+* mice; (iii) non-diabetic *db/+ eNOS* *-/-* mice; (iv) non-  
121 diabetic *db/+ eNOS* *+/+* mice. Breeding pairs of *db/+ eNOS* *-/-* mice were obtained from The  
122 Jackson Laboratory (Jax # 8340, Bar Harbor, ME, USA) and experimental groups were derived  
123 from mating *db/+ eNOS* *-/-* to *db/+ eNOS* *+/+* mice. Mice were fed a standard diet (Lab Diet  
124 5L0D, 58% calories from carbohydrate, 13.5% calories from fat, and 28.5% calories from protein,  
125 Brentwood, MO, USA) and housed in a pathogen-free environment by personnel in the University  
126 of Michigan Unit for Laboratory Animal Medicine. Approximately, half of the mice of each  
127 genotype were treated with a combination of RAS blockers, lisinopril 20 mg/day and losartan 30  
128 mg/day in drinking water, from 10-12 wks to 26 wks of age. There were no adverse effects from  
129 the treatment. All animal procedures were in accordance with the policies of the University of  
130 Michigan Institutional Animal Care and Use Committee.

131 Metabolic phenotyping.

132 For each animal, body weight and fasting blood glucose (FBG; AlphaTrak Glucometer, Abbott  
133 Laboratories, Abbott Park, IL, USA) were measured weekly. Prior to euthanasia, spot urines were  
134 collected. At study termination, glycated hemoglobin (GHb) levels, plasma cholesterol, and  
135 triglycerides were measured by the Michigan Diabetes Research Center Chemistry Laboratory.  
136 Kidney tissue and dorsal root ganglia (DRG) were rapidly extracted and glomeruli from one kidney  
137 were iron-perfused and magnetically isolated as previously reported (20, 21).

138 DKD and DPN phenotyping.

139 All animals were phenotyped for DKD and DPN according to Diabetic Complications Consortium  
140 guidelines (<https://www.diacomp.org>), as previously published (22, 23). Glomerular area was  
141 determined using Periodic acid Schiff (PAS) staining (21, 24, 25). Briefly, 15 glomerular tufts per  
142 mouse were randomly selected and the percent glomerular area that was PAS-positive was  
143 calculated. Quantification was performed with MetaMorph (version 6.14). Urinary albumin  
144 concentration was determined by ELISA (Albuwell, Exocell, Philadelphia, PA, USA) and urinary  
145 creatinine levels with a color endpoint reagent (C513-480, Teco Diagnostics, Anaheim, CA, USA),  
146 as previously reported (26). Sensory (sural) and motor (sciatic) nerve conduction velocities

147 (NCVs) were measured for large nerve fiber function (13, 27, 28). Sural NCVs were measured by  
148 recording at the dorsum of the foot and exerting an antidromic supramaximal stimulation at the  
149 ankle. Sural NCVs were calculated by dividing the distance between the recording and stimulating  
150 electrodes by the onset latency of the sensory nerve action potential. Sciatic NCVs were measured  
151 by recording at the dorsum of the foot and exerting an orthodromic supramaximal stimulation first  
152 at the ankle, then at the sciatic notch. Sciatic NCVs were calculated by dividing the distance  
153 between the two stimulation sites by the difference between the two onset latencies.

154 Phenotypic data were presented as means  $\pm$  standard error of the mean. Group numbers  
155 were unequal due to group births frequency. For kidney phenotyping, 5 random animals/group  
156 were identified. All phenotypic data were analyzed in 5 pair-wise comparisons involving a total of  
157 6 groups of mice based on a priori selection of the statistical comparisons (diabetic *db/db eNOS* -  
158 */-* mice treated and untreated; diabetic *db/db eNOS* *+/+* mice treated and untreated; non-diabetic  
159 *db/+ eNOS* *-/-* mice untreated; and non-diabetic *db/+ eNOS* *+/+* mice untreated). Statistical  
160 analyses were performed using GraphPad Prism Software (Version 7, GraphPad, La Jolla, CA,  
161 USA). Comparisons between multiple groups were performed using one-way ANOVA with  
162 Tukey's post-test or Kruskal-Wallis test with Dunn's post-test for multiple comparisons.  
163 Significance was assigned when  $p < 0.05$ .

#### 164 RNA sequencing (RNA-seq).

165 Kidney glomeruli analysis consisted of subsets of all groups (which included all animals that  
166 underwent metabolic, DKD, and DPN phenotyping, plus several animals from each group that  
167 had undergone all phenotyping except kidney glomerular morphometry): *db/+ eNOS* *+/+* ( $n =$   
168 10), *db/db eNOS* *+/+* ( $n = 7$ ), *db/+ eNOS* *+/+* treated ( $n = 10$ ), and *db/db eNOS* *+/+* treated ( $n =$   
169 11), *db/+ eNOS* *-/-* ( $n = 10$ ), *db/db eNOS* *-/-* ( $n = 9$ ), *db/+ eNOS* *-/-* treated ( $n = 10$ ), and *db/db*  
170 *eNOS* *-/-* treated ( $n = 7$ ) mice. For DRG, we included subsets of *db/db eNOS* *-/-* untreated ( $n = 5$ ),  
171 and *db/db eNOS* *-/-* treated ( $n = 4$ ) mice (all of which had undergone metabolic, DKD and DPN  
172 phenotyping). RNA was obtained using the RNeasy Mini Kit (Qiagen, Hilden, Germany) and  
173 quality was assessed using TapeStation (Agilent, Santa Clara, CA, USA). Samples with RNA  
174 integrity numbers  $\geq 8$  were prepared using TruSeq mRNA Sample Prep v2 kit (Illumina, San  
175 Diego, CA, USA). Paired end 101 bp RNA sequencing was performed by the University of  
176 Michigan DNA Sequencing Core (<http://seqcore.brcf.med.umich.edu/>).

177 For quality control, the raw reads were assessed using the FastQC tool  
178 (<http://www.bioinformatics.babraham.ac.uk/projects/fastqc/>) (Supplements, FastQC.zip). A  
179 randomly selected set of reads was mapped against several potential artifacts using the  
180 FastqScreen tool ([https://www.bioinformatics.babraham.ac.uk/projects/fastq\\_screen/](https://www.bioinformatics.babraham.ac.uk/projects/fastq_screen/))  
181 (Supplements, QC.pdf). The first 14 bases of the reads were clipped with the FASTX toolkit  
182 ([http://hannonlab.cshl.edu/fastx\\_toolkit/](http://hannonlab.cshl.edu/fastx_toolkit/)). Mapping statistics, hierarchical clustering, PCA,  
183 FastQC results, and FastqScreen were combined to identify samples that consistently show  
184 abnormalities, such as samples with rRNA mapping rates  $\geq 10\%$ . Then, RNA-seq data were  
185 analyzed using the Tuxedo suite, including Bowtie 2, TopHat 2, and Cufflinks (29). Using  
186 TopHat, the resulting FASTQ files were aligned to the NCBI reference mouse transcriptome  
187 (NCBI 37.2) to identify known transcripts. Mapped reads were processed using the Cufflinks  
188 pipeline to calculate fragments per kilobase of exon per million mapped reads (FPKM) (29). This  
189 pipeline aggregated transcript FPKM data to gene level abundance estimates, which were used  
190 for further analysis. The RNA-seq data are deposited in the Gene Expression Omnibus database  
191 ([www.ncbi.nlm.nih.gov/geo](http://www.ncbi.nlm.nih.gov/geo)) under accession number GSE159060.

#### 192 Pair-wise comparison.

193 Pair-wise comparison was performed on 2 of the DKD and the DPN datasets. The output of  
194 Cufflinks was loaded into Cuffdiff (29) to determine differences in transcript abundance  
195 estimates in binary comparisons. For kidney tissue, analyses focused on *db/+* vs. *db/db* and  
196 *db/db* vs. *db/db eNOS<sup>-/-</sup>* differentially expressed gene (DEG) to identify gene expression  
197 changes in *db/db* mice that were altered or unaffected by *eNOS* knockout. For nerve tissue, we  
198 restricted transcriptomic analysis to the effect of RAS blockade in *db/db eNOS<sup>-/-</sup>* animals.  
199 DEGs were defined as those with a false discovery rate adjusted p-value (q-value) cutoff  $< 0.05$ .

#### 200 Self-organizing map (SOM) analysis.

201 A SOM is a type of artificial neural network that generates a two-dimensional grid and clusters,  
202 in an unbiased manner, similar patterns of gene expression into units called modules. Genes with  
203  $< 2$  FPKM were considered as not expressed and removed from the analysis. The FPKMs for the  
204 remaining genes were  $\log_2$  transformed. The average expression values for each group were  
205 centered at zero, and SOM was applied using the algorithm implemented in the MATLAB  
206 software Neural Networking toolbox (<https://www.mathworks.com/products/neural->

207 [network.html](#)) (MathWorks, Natick, MA, USA). Gene sets with similar expression patterns were  
208 grouped into modules, and each module was subjected to functional enrichment analysis.  
209 Adjacent modules were further combined into clusters that shared enriched functions and similar  
210 gene expression patterns. SOM analysis was only performed on the DKD dataset, and not on  
211 nerve datasets, since *eNOS* knockout or treatment did not affect the DPN phenotype.

## 212 Functional enrichment analysis.

213 Hierarchical clustering based on significance values was used to represent overall similarity and  
214 differences between the DKD DEG sets (19). Over-represented biological functions from the  
215 DPN DEG sets were identified by functional enrichment analysis using Ingenuity Pathways  
216 Analysis software (IPA, QIAGEN, Redwood City, CA, USA) (30). Functional analysis on SOM  
217 module units was performed using gene ontology (31) (<http://www.geneontology.org/>). A  
218 Benjamini-Hochberg adjusted p-value was calculated using the Fisher's exact test and p-values <  
219 0.05 were used to identify significantly over-represented gene ontology terms.

220

## 221 **Results**

### 222 Metabolic phenotyping

223 The metabolic measurements for all experimental groups are summarized in Table 1. The *db/db*  
224 mice were significantly heavier than *db/+* mice at study termination, and *eNOS* deletion did not  
225 affect body weight. Blood glucose and GHb were significantly higher in *db/db* mice compared to  
226 *db/+* mice, and were not affected by *eNOS* knockout. Total plasma cholesterol and triglyceride  
227 levels were significantly greater in the *db/db eNOS -/-* versus *db/+ eNOS -/-* mice. Kidney weight  
228 significantly increased in *db/db* compared to *db/+* mice, and in *db/db eNOS -/-* versus *db/+ eNOS*  
229 *-/-* mice, an effect RAS inhibitor therapy did not further impact.

### 230 DKD phenotyping

231 Urine volumes (Fig. 1A) and albuminuria (Fig. 1B) significantly increased in *db/db* compared to  
232 *db/+* mice, but were not affected by RAS blockade in either group. There was a major increase in  
233 albuminuria in the *db/db eNOS -/-* mice versus all other groups, which was significantly attenuated  
234 by RAS blockade (Fig. 1B).

235 Mesangial expansion as denoted by glomerular PAS-positive area significantly increased  
236 in *db/db* mice compared to *db/+* mice (Fig. 1C), but was not affected by RAS inhibition in either



237 group, as with albuminuria. There was a further non-significant increase in mesangial expansion  
238 in the *db/db eNOS*<sup>-/-</sup> mice versus all other groups, which was significantly attenuated by RAS  
239 blockade (Fig. 1C). The percentage of globally sclerotic glomeruli was also significantly increased  
240 in the *db/db eNOS*<sup>-/-</sup> mice compared to *db/db* mice (Fig. 1D). RAS inhibition had a trending  
241 reduction in the number of globally sclerotic glomeruli but this was not statistically significant due  
242 to large variances.

#### 243 DPN phenotyping

244 The *db/db* mice had significantly delayed sural (Fig. 2A) and sciatic (Fig. 2B) NCVs, which were  
245 not further affected by *eNOS* knockout. Interestingly, RAS inhibition did not impact NCVs in  
246 either *db/db* or *db/db eNOS*<sup>-/-</sup> animals compared to their respective control littermates. Hind paw  
247 withdrawal latency was abnormally increased in *db/db* animals compared to *db/+* mice. *eNOS*  
248 knockout did not affect hind paw withdrawal latency independent of the diabetes status (Fig. 2C).

#### 249 Differential expression analysis in isolated glomeruli

250 The experimental design integrated three experimental variables (diabetes status, *eNOS* dosage,  
251 and RAS inhibition), which resulted in 8 groups for comparison in DKD analysis. Hierarchical  
252 gene expression clustering (Fig. 3A) showed that groups that were similar in gene expression were  
253 also similar in disease severity (Fig. 3B). Diabetes had a more substantial effect on glomerular  
254 gene expression than *eNOS* knockout, as diabetic groups had more abnormal gene expression  
255 profile than nondiabetic groups (Fig. 3A). This is similar to the relative effects of diabetes and  
256 *eNOS* knockout on the DKD phenotype, as *eNOS* knockout alone had very little independent effect  
257 on glomerular pathology or albuminuria, whereas diabetes had a major effect on DKD,  
258 independent of *eNOS* expression (Fig. 1). Interestingly, RAS inhibition improved the DKD  
259 phenotype (Fig. 1), but moved the gene expression profile in the opposite direction, towards a  
260 more abnormal transcriptional pattern (Fig. 3A and B). This was not due to lack of RAS blockade,  
261 because DEG sets pointed towards functional inhibition of angiotensin converting enzyme and  
262 blockade of angiotensin receptors (e.g., increased renin gene expression, not shown).

#### 263 SOM analysis

264 Using SOM analysis, we examined changes in transcriptional patterns of kidney glomeruli across  
265 the 8 experimental groups. This approach comprehensively clustered the transcriptomic data in an

266 unbiased manner based on the similarity between their sequential expression profiles. All genes  
267 were projected onto a SOM consisting of a 7 x 7 map of modules (Fig. 4A and 4B). Each module  
268 (Fig. 4A) displays a unique pattern of gene expression across the 8 experimental groups.

269 As noted in the upper left portion of the glomerular SOM (Figs. 4A, 4B, and 4C), 1403  
270 genes were coordinately decreased in *db/db eNOS* *-/-* mouse glomeruli in the indicated clusters,  
271 consisting of adjacent modules with similar patterns in gene expression. These genes were most  
272 highly expressed in the phenotypically normal group, *db/+ eNOS* *+/+* mice, and decreased with  
273 worsening disease across the 8 groups. Highly prevalent among these genes were transcription  
274 factors that regulate metabolic and developmental processes, including fatty acid metabolism and  
275 nephron development (Supplemental Table 1). However, not all podocyte-specific genes showed  
276 this pattern. For example, nephrin (*Nphs1*) gene expression was fairly constant across 6 of the  
277 groups but was moderately and similarly decreased in the two *eNOS* *-/-* diabetic groups  
278 (Supplemental Fig. 1A). On the other hand, canonical transient receptor potential-6 channels  
279 (*Trpc6*) gene was expressed at equivalent levels across all groups (Supplemental Fig. 1B). As  
280 predicted from the SOM, developmental gene expression also significantly decreased in the  
281 pairwise transcriptomic comparison of *eNOS* *-/- db/db* vs. *eNOS* *+/+ db/+* mice (Supplemental  
282 Table 2). Regulated genes of interest included those encoding growth factors, such as platelet-  
283 derived growth factor receptor beta (*Pdgfrb*) and neuronal growth regulator 1 (*Negr1*), previously  
284 implicated in murine and human DKD development (32, 33).

285 As shown in the lower right portion of the SOM panel (Fig. 4), 1354 genes were  
286 coordinately elevated in *db/db eNOS* *-/-* glomeruli in the indicated cluster. These genes were  
287 expressed at the lowest levels in the phenotypically normal group, *db/+ eNOS* *+/+* mice, and  
288 increased with worsening disease across the 8 mouse groups. Most significant upstream regulators  
289 in these clusters were associated with inflammation using IPA (Supplemental Table 3). As  
290 predicted from the SOM, inflammatory signaling gene expression also significantly increased in  
291 the pairwise transcriptomic comparison of *db/db eNOS* *-/-* vs. *db/+ eNOS* *+/+* mice, with top DEGs  
292 including NLR family, pyrin domain containing 3 (*Nlrp3*) and tumor necrosis factor (*Tnf*), key  
293 players in DKD pathogenesis (Supplemental Table 4) (34, 35).

294 Fibrotic pathways were also represented in the SOM analysis, though they were not as  
295 prominent as the inflammatory pathways. Analysis of SOM clusters that showed a similar pattern  
296 of enhanced gene expression across the disease spectrum in the 8 experimental groups (as indicated

297 in Fig. 4D) showed progressive enrichment of the hepatic fibrosis/hepatic stellate activation  
298 pathway (enrichment  $p=3.98E-06$ ) moving from the least diseased to the most diseased mouse  
299 model (*data not shown*). Assessment of the genes coordinately up-regulated in the most diseased  
300 phenotype (*db/db eNOS*<sup>-/-</sup> mice) indicated enrichment of the hepatic fibrosis/hepatic stellate  
301 canonical pathway ( $p=3.16E-16$ ). Upregulated pro-fibrotic genes included: *ACTA2*, *MMP2*,  
302 *MMP9*, *COL1A1*, *COL12A1*, *FNI*, *TGFB1*, *COL4A1*, *COL3A1*, *COL8A1*, *MMP13*, *COL4A2*,  
303 *TIMP1*, *SERPINE1*, *COL13A1*, *ICAM1*, *PDGFA*. These findings supported enrichment of this pro-  
304 fibrotic pathway and enrichment for genes downstream of TGFB1 (enrichment  $p=4.06E-30$ ).  
305 Finally, we investigated the correlation between both albuminuria and mesangial index and SOM  
306 gene expression in the two most extreme modules (1,1 and 7,7 on the upper left and lower right  
307 SOM corners, respectively). There was a statistically significant correlation between aggregate  
308 gene expression from each of these modules with both albuminuria and mesangial index, two  
309 major components of DKD severity (Fig. 5).

#### 310 Transcriptomics data analysis in isolated DRG

311 *eNOS* knockout did not affect DPN phenotype and transcriptomic analysis of neuropathic changes  
312 in *db/db* mice was recently published (36, 37); thus, we restricted transcriptomic analysis of DRG  
313 to the effect of RAS inhibition in *db/db eNOS*<sup>-/-</sup> animals. This pairwise analysis showed that  
314 treatment enhanced expression of several genes known to play a pathogenic role in DPN (36-38),  
315 including members of the pro-oxidant NADPH oxidase family (*Cybb/ Nox2*) as well as matrix  
316 metalloproteinase *Mmp-2* and *Mmp-9* (Fig. 6). Additionally, top inflammatory DEGs included  
317 complement component factor h (*Cfh*), previously implicated in the development of human DPN  
318 (Supplemental Table 5) (39). To identify the overrepresented biological pathways among these  
319 regulated genes, functional enrichment analysis of DEGs was carried out using IPA. Our analysis  
320 showed that multiple pathways involved in inflammation, oxidative stress, and fibrotic processes  
321 were significantly enriched in mice treated with RAS blockers (Fig. 6). This includes hepatic  
322 fibrosis/hepatic stellate cell activation, which we previously found enriched in *db/db* mice through  
323 the course of DPN (36). Besides *Cybb/ Nox2*, top DEGs involved in nitric oxide and reactive  
324 oxygen species production in macrophages pathway included *Stat1*, a regulator of NADPH  
325 oxidase-derived oxidant production, including *Nox2* (Supplemental Table 6) (40).

326

#### 327 **Discussion**

328 Using a genome-wide expression analysis of kidney glomeruli and DRG tissues, we evaluated the  
329 impact of type 2 diabetes (due to a leptin receptor mutation) and *eNOS* deletion on DKD and DPN  
330 severity. Both diabetes and *eNOS* deletion contributed to phenotypic severity and molecular profile  
331 alterations of glomerulopathy in DKD, whereas DPN progression and nerve gene expression were  
332 mostly affected by diabetes status only. This confirms our previous findings that DPN versus DKD  
333 pathogenesis differ significantly (8, 9, 41). Also consistent with our previous reports (8, 41),  
334 treatment with standard-of-care RAS inhibitors, lisinopril and losartan, ameliorated DKD, but not  
335 DPN, suggesting that a ‘one size fits all’ therapeutic strategy does not work for all type 2 diabetic  
336 complications. By using a SOM approach and conventional hierarchical clustering of  
337 transcriptomic differences, we found that certain gene expression profiles related to podocyte  
338 integrity and pro-inflammatory pathways sequentially changed with increasing DKD severity from  
339 non-diabetic mice through modest glomerulopathy in *eNOS* *-/-* animals, to more severe decline in  
340 diabetic *eNOS* *+/+* animals, and the greatest change in the most diseased group, diabetic *eNOS* *-/-*  
341 mice. Although RAS inhibition improved the DKD phenotype, it did not impact the dysfunctional  
342 gene expression pattern in kidney and exacerbated it in nerve, enhancing expression of genes  
343 involved in inflammation and oxidant generation. It is clear that RAS inhibition monotherapy or  
344 combination therapy provides inadequate protection in humans with DKD. Nonetheless, combined  
345 RAS inhibition does provide substantial reduction in disease manifestations in rodents (42), so it  
346 is remarkable that the transcriptomic parameters failed to improve and actually worsened in this  
347 setting. Overall, these analyses shed new light onto specific pathogenic pathways underlying DKD  
348 and DPN, emphasize the inefficacy of RAS blockade in correcting abnormal gene expression in  
349 DKD and DPN, and offer specific pro-inflammatory and pro-oxidant candidates for developing  
350 complication-specific therapeutics.

351 The *db/db eNOS* *-/-* mouse has been well characterized over the past 10-15 years as one of  
352 the most robust DKD models (12, 43). Since both diabetes status (*db* allele) and *eNOS* deficiency  
353 were genetically determined, it was possible to separate out each of these factors based on animal  
354 genotype from a single breeding colony. Genome-wide expression differences between animals  
355 that co-segregate by genotype for the *db* (leptin receptor) and/or *eNOS* genes allowed us to  
356 determine which of these two underlying factors was responsible for the gene expression changes.  
357 In that regard, it is of interest that both diabetes status and *eNOS* deletion appeared to separately  
358 and additively result in gene expression changes that associate with the DKD phenotype. Further,

359 the expression of genes that most clearly increased or decreased with phenotype severity also  
360 correlated with both albuminuria and mesangial expansion, two major DKD features. Our findings  
361 show that diabetes per se had a more prominent effect on kidney injury, but *eNOS* deletion  
362 accelerated the phenotype, as has been recently suggested by Azushima et al. (43).

363 While the tight correlation between transcriptomic changes and phenotype might seem a  
364 predictable result, there are many examples where progressive gene expression differences are not  
365 associated with clinical phenotypic differences or, conversely there are many examples where  
366 progressive changes in phenotype are not associated with gene expression differences (44, 45). In  
367 fact, it is rare for graded gene expression phenotypes to parallel graded disease phenotypes, as  
368 there is often a threshold effect of gene expression changes on disease phenotype (45). Thus, this  
369 parallel between graded gene expression changes and graded phenotypic differences was striking  
370 and uncommon.

371 Another prominent finding was the predominance of pro-inflammatory gene expression,  
372 which increased along the spectrum from the most normal to the most diseased groups in the SOM  
373 analysis. These gene expression changes were mediated by both diabetes and *eNOS* deficiency,  
374 since each individually increased inflammatory gene expression, and combined exacerbated the  
375 response. Among these genes, *Nlrp3* is an interesting candidate because Nlrp3 inflammasome has  
376 been reported to be a critical player in initiating the early stages of glomerular and tubulointerstitial  
377 inflammation and its activation correlates with DKD severity in experimental and clinical diabetes  
378 (34, 46, 47). Similarly, we observed increased *Tnf*, which has been shown to amplify cytokine  
379 production, thus enhancing the existing inflammatory response, exacerbating oxidative stress, and  
380 promoting a stronger DKD phenotype (48, 49). Of all the genes that followed this pattern,  
381 inflammatory genes such as *Nlrp3* and *Tnf* were the most prominent, strongly suggesting that  
382 inflammatory processes are not simply one of many pathways that augment DKD, but the  
383 predominant process, at least in this model. A role for activated immune and inflammatory  
384 responses with increases in pro-inflammatory mediators like *Tnf* has also been reported in other  
385 mouse models of DKD including the Akita-RenTg mice that develop both type 1 diabetes and a  
386 robust kidney disease phenotype (50). Similar transcriptomic data were also observed in the  
387 glomeruli of streptozotocin-induced type 1 diabetic mice (51). In addition, we previously  
388 compared the glomerular transcriptomic changes in three of the best murine DKD models  
389 (*C57BLKS db/db eNOS<sup>-/-</sup>*, streptozotocin DBA/2 and *C57BLKS db/db*) to early human DKD and

390 found consistent increases in inflammatory pathways in all 3 models that overlapped with those in  
391 humans. This was despite the fact that pathway overlap in general with the human disease  
392 transcriptome was only moderately good. In that analysis, the *db/db eNOS -/-* model had the most  
393 overlap with human disease pathways compared to all other models (44). Thus, these results not  
394 only support our findings, but also suggest that the immune response may be a causal factor in  
395 human DKD pathogenesis regardless of diabetes type.

396 We also observed a progressive reduction in podocyte and developmental gene expression  
397 as the pathologic features increased across the 8 experimental groups. This pattern was striking  
398 and generally confirmed the gradual reduction in some podocyte-specific genes and pathways in  
399 progressive DKD. Previous reports of murine DKD models have demonstrated reduced expression  
400 of podocyte and differentiation genes in some, though not all, mouse DKD models (44, 52).  
401 Although RAS inhibition has been found to ameliorate some of the podocyte-specific gene  
402 expression changes in some mouse models (52), it had no effect on the SOM-identified gene  
403 expression modules that tracked most closely with the disease process, suggesting that RAS  
404 inhibition was not particularly effective at preserving podocyte molecular physiology.

405 Perhaps most surprising in this analysis was that ameliorative RAS blockade treatment did  
406 not alleviate gene expression abnormalities, including increases in inflammatory genes, as  
407 evidenced by both the hierarchical clustering and the SOM analysis. Although it has been reported  
408 that RAS blockade has anti-inflammatory properties (53), it seems likely, at least in this model,  
409 that its salutary effects were not due to anti-inflammatory mechanisms (54). In agreement with our  
410 current data, anti-inflammatory RAS blockade mechanisms have been shown to be reduced by  
411 angiotensin and aldosterone “breakthrough”, as well as by blocking anti-inflammatory aspects of  
412 angiotensin signaling via Ang (1-7) and other aspects of this complex signaling pathway (54).  
413 Thus, our results suggest that RAS blockade influences other gene expression modules that are not  
414 so prominent in the underlying disease progression, but still have a beneficial effect on disease  
415 phenotype (55). Yet, if inflammation is the key driving process, at least in early DKD (56), the  
416 lack of reversal of underlying inflammatory gene expression changes may explain why RAS  
417 blockade only modestly slowed DKD progression and failed to halt it.

418 Given the range of nephropathy phenotypes among the 8 experimental groups, the SOM  
419 analysis was quite informative as it automatically grouped genes together whose expression  
420 directly or inversely correlated with DKD severity. This map showed significantly and sequentially

421 enhanced inflammatory gene profiles, and sequentially reduced podocyte-specific, metabolic, and  
422 developmental gene profiles with progressive DKD. This gives increasing credence to the growing  
423 evidence on the importance of low-grade inflammation on DKD progression across the disease  
424 spectrum (57, 58). Moreover, it suggests that developmental and metabolic gene expression is  
425 critical for normal kidney function and that maintained expression of specific glomerular cell genes  
426 may help prevent disease progression. Among these mechanisms, fatty acid and cellular lipid  
427 metabolic dysregulation are of particular interest because lipid abnormalities are increasingly  
428 recognized by our group and others as independent risk factors for DKD development (59-61).  
429 Importantly, these results are also consistent with recent findings in multiple type 2 diabetic mouse  
430 models such as the KK-Ay mouse (62) and the BTBR *ob/ob* leptin-deficient mouse (63), further  
431 reinforcing our data. Since our findings in this report show association and not causality, direct  
432 effects of these increased and decreased gene expression changes will need to be verified  
433 experimentally.

434 In contrast to the graded increase with DKD, DPN was not affected by either *eNOS* deletion  
435 or RAS inhibition. There was a substantial effect of diabetes on both the DPN phenotype and on  
436 gene expression changes, similar to recent findings by our group in *db/db* animals (36, 37), and in  
437 DPN patients (64, 65). Also in agreement with our previous findings (36, 37), pairwise analysis  
438 showed that diabetes was associated with a significant increase in inflammatory pathways and  
439 immune system activation. Current and previous data point to the immune system as a major  
440 pathogenic factor in DPN, with the innate immune system in a central role (9, 36). Similar  
441 inflammatory and immune system pathways were activated in nerve tissue and glomeruli in *db/db*  
442 *eNOS* *-/-* mice. Interestingly, RAS blockade exacerbated DPN gene expression patterns and  
443 enriched nerve DEGs in molecular pathways related to inflammatory and oxidative stress  
444 responses as well as fibrotic processes. Within these enriched pathways, *Cybb/ Nox2* was a  
445 particularly interesting DEG because of its role in oxidant generation in DPN (38) and contribution  
446 to neuropathic pain and pro-inflammatory cytokine expression in peripheral nerves (66, 67).  
447 Indeed, these reports are aligned with our current results, in turn suggesting that *Cybb/ Nox2*  
448 overexpression following RAS blockade may intensify an already activated oxidative environment  
449 in *db/db eNOS* *-/-* nerves, which may at least partly explain why treatment did not improve nerve  
450 function. Other pathways RAS inhibition exacerbated in DRGs included integrin-linked kinase  
451 (ILK) signaling, which is associated with the development of insulin resistance and apoptosis in

452 complication-prone tissues, including neuronal tissue (68-70). Of note, top upregulated genes  
453 within this pathway included *Mmp-9*, a modulator of neuropathic pain, whose inhibition reduces  
454 microglial activation and nerve injury (71, 72). In the presence of diabetes, MMP-9 has been found  
455 to be upregulated in sciatic nerves of STZ-induced type 1 diabetic rats (73), and implicated in  
456 regeneration at the site of nerve injury (74). Interestingly, *Mmp-9*, through its interaction with *Ilk*,  
457 induces glomerular hypertrophy and DKD, and a similar mechanism may be occurring in DPN  
458 based on our findings (75). Taken together, we propose that RAS blockade by enhancing processes  
459 like Nox2-dependent oxidative stress and pro-inflammatory and fibrotic processes such as ILK  
460 signaling, likely contribute to the lack of treatment effect on nerve function in the *db/db eNOS -/-*  
461 mouse.

462 In summary, careful phenotypic and transcriptomic analysis of an excellent mouse model  
463 of diabetic glomerulopathy has shed new light on molecular DKD pathogenesis, implicating a  
464 network of gene expression alterations, especially in developmental, metabolic, and inflammatory  
465 pathways, that predicts progressive changes characteristic of early DKD. Since these changes were  
466 identified through an unbiased mapping tool that describes underlying structure without imposing  
467 a preconceived hierarchy, such gene expression changes are likely fundamental to the DKD  
468 phenotype. Another striking feature of this analysis was that RAS blockers worsened DKD gene  
469 expression profiles, confirming their inadequacy as a DKD treatment. While a similarly complete  
470 transcriptomic analysis could not be performed for DPN, since neither *eNOS* deletion nor RAS  
471 blockade altered the disease process, we found that RAS blockade activated pro-oxidant and  
472 inflammatory gene expression very similar to that by diabetes, *eNOS* deletion, and RAS blockade  
473 in DKD. These findings support our previous reports of inflammatory pathway activation as key  
474 to the pathogenesis of both complications (9, 36) and suggest that early DKD and DPN could be  
475 effectively treated by specific anti-inflammatory strategies.

476

#### 477 **Acknowledgments**

478 Funding was provided by the National Institutes of Health (NIH) (1DP3DK094292, 1R24082841  
479 to S.P., J.H., M.K., E.L.F., and F.C.B.); Novo Nordisk Foundation (NNF14OC0011633 to E.L.F.  
480 and L.M.H.), the Nathan and Rose Milstein Research Fund (to S.A.E), Neuronetwork for  
481 Emerging Therapies at the University of Michigan (to S.A.E. and E.L.F.), and the A. Alfred  
482 Taubman Medical Research Institute (to S.A.E. and E.L.F.). Research reported in this study was



483 also made possible by Core Services supported by the National Institute of Diabetes and  
484 Digestive Kidney Diseases (NIDDK) of the NIH under award number U2CDK110768 (MMPC)  
485 and by the University of Michigan O'Brien Kidney Translational Core Center funded by the NIH  
486 (2P30DK081943).

487

#### 488 **Conflict of Interest**

489 The authors have stated explicitly that there are no conflicts of interest in connection with this  
490 article.

#### 491 **Author Contributions**

492 S.A.E. and L.M.H. wrote the manuscript, contributed to discussion and researched data, H.Z.,  
493 R.E, V.N., S.E., F.E., and M.P. researched data, contributed to discussion, and reviewed/edited  
494 the manuscript, J.S., and C.C.B. researched data and contributed to discussion, H.V.J, Y.G., S.P.,  
495 J.H., M.K., and E.L.F. contributed to discussion and reviewed/edited the manuscript. F.C.B  
496 contributed to discussion and wrote the manuscript. E.L.F. and F.C.B. are the guarantors of this  
497 work and, as such, had full access to all the data in the study and take responsibility for the  
498 integrity of the data and the accuracy of the data analysis.

499

500

#### 501 **References**

- 502 1. Saran, R., Robinson, B., Abbott, K. C., Agodoa, L. Y. C., Bragg-Gresham, J.,  
503 Balkrishnan, R., Bhave, N., Dietrich, X., Ding, Z., Eggers, P. W., Gaipov, A., Gillen,  
504 D., Gipson, D., Gu, H., Guro, P., Haggerty, D., Han, Y., He, K., Herman, W., Heung,  
505 M., Hirth, R. A., Hsiung, J. T., Hutton, D., Inoue, A., Jacobsen, S. J., Jin, Y., Kalantar-  
506 Zadeh, K., Kapke, A., Kleine, C. E., Kovesdy, C. P., Krueter, W., Kurtz, V., Li, Y., Liu,  
507 S., Marroquin, M. V., McCullough, K., Molnar, M. Z., Modi, Z., Montez-Rath, M.,  
508 Moradi, H., Morgenstern, H., Mukhopadhyay, P., Nallamothu, B., Nguyen, D. V.,  
509 Norris, K. C., O'Hare, A. M., Obi, Y., Park, C., Pearson, J., Pisoni, R., Potukuchi, P. K.,  
510 Repeck, K., Rhee, C. M., Schaubel, D. E., Schragger, J., Selewski, D. T., Shamraj, R.,

- 511 Shaw, S. F., Shi, J. M., Shieu, M., Sim, J. J., Soohoo, M., Steffick, D., Streja, E.,  
512 Sumida, K., Kurella Tamura, M., Tilea, A., Turf, M., Wang, D., Weng, W., Woodside,  
513 K. J., Wyncott, A., Xiang, J., Xin, X., Yin, M., You, A. S., Zhang, X., Zhou, H., and  
514 Shahinian, V. (2019) US Renal Data System 2018 Annual Data Report: Epidemiology  
515 of Kidney Disease in the United States. *Am J Kidney Dis* **73**, A7-A8
- 516 2. Leoncini, G., Viazzi, F., De Cosmo, S., Russo, G., Fioretto, P., and Pontremoli, R.  
517 (2020) Blood pressure reduction and RAAS inhibition in diabetic kidney disease:  
518 therapeutic potentials and limitations. *J Nephrol*
- 519 3. Feldman, E. L., Callaghan, B. C., Pop-Busui, R., Zochodne, D. W., Wright, D. E.,  
520 Bennett, D. L., Bril, V., Russell, J. W., and Viswanathan, V. (2019) Diabetic  
521 neuropathy. *Nat Rev Dis Primers* **5**, 41
- 522 4. Callaghan, B. C., Price, R. S., and Feldman, E. L. (2020) Distal Symmetric  
523 Polyneuropathy in 2020. *JAMA* **324**, 90-91
- 524 5. Juster-Switlyk, K., and Smith, A. G. (2016) Updates in diabetic peripheral neuropathy.  
525 *F1000Res* **5**
- 526 6. Komorowsky, C. V., Brosius, F. C., 3rd, Pennathur, S., and Kretzler, M. (2012)  
527 Perspectives on systems biology applications in diabetic kidney disease. *J Cardiovasc*  
528 *Transl Res* **5**, 491-508
- 529 7. Feldman, E. L., Nave, K. A., Jensen, T. S., and Bennett, D. L. H. (2017) New Horizons  
530 in Diabetic Neuropathy: Mechanisms, Bioenergetics, and Pain. *Neuron* **93**, 1296-1313
- 531 8. Hinder, L. M., Park, M., Rumora, A. E., Hur, J., Eichinger, F., Pennathur, S., Kretzler,  
532 M., Brosius, F. C., 3rd, and Feldman, E. L. (2017) Comparative RNA-Seq  
533 transcriptome analyses reveal distinct metabolic pathways in diabetic nerve and kidney  
534 disease. *J Cell Mol Med* **21**, 2140-2152
- 535 9. Hur, J., O'Brien, P. D., Nair, V., Hinder, L. M., McGregor, B. A., Jagadish, H. V.,  
536 Kretzler, M., Brosius, F. C., 3rd, and Feldman, E. L. (2016) Transcriptional networks of  
537 murine diabetic peripheral neuropathy and nephropathy: common and distinct gene  
538 expression patterns. *Diabetologia*
- 539 10. King, A. J. (2012) The use of animal models in diabetes research. *Br J Pharmacol* **166**,  
540 877-894

- 541 11. O'Brien, P. D., Sakowski, S. A., and Feldman, E. L. (2014) Mouse models of diabetic  
542 neuropathy. *ILAR J* **54**, 259-272
- 543 12. Brosius, F. C., 3rd, Alpers, C. E., Bottinger, E. P., Breyer, M. D., Coffman, T. M.,  
544 Gurley, S. B., Harris, R. C., Kakoki, M., Kretzler, M., Leiter, E. H., Levi, M., McIndoe,  
545 R. A., Sharma, K., Smithies, O., Susztak, K., Takahashi, N., and Takahashi, T. (2009)  
546 Mouse models of diabetic nephropathy. *J Am Soc Nephrol* **20**, 2503-2512
- 547 13. Hinder, L. M., O'Brien, P. D., Hayes, J. M., Backus, C., Solway, A. P., Sims-Robinson,  
548 C., and Feldman, E. L. (2017) Dietary reversal of neuropathy in a murine model of  
549 prediabetes and metabolic syndrome. *Dis Model Mech* **10**, 717-725
- 550 14. Zhao, H. J., Wang, S., Cheng, H., Zhang, M. Z., Takahashi, T., Fogo, A. B., Breyer, M.  
551 D., and Harris, R. C. (2006) Endothelial nitric oxide synthase deficiency produces  
552 accelerated nephropathy in diabetic mice. *J Am Soc Nephrol* **17**, 2664-2669
- 553 15. Nakagawa, T., Sato, W., Glushakova, O., Heinig, M., Clarke, T., Campbell-Thompson,  
554 M., Yuzawa, Y., Atkinson, M. A., Johnson, R. J., and Croker, B. (2007) Diabetic  
555 endothelial nitric oxide synthase knockout mice develop advanced diabetic  
556 nephropathy. *J Am Soc Nephrol* **18**, 539-550
- 557 16. Kanetsuna, Y., Takahashi, K., Nagata, M., Gannon, M. A., Breyer, M. D., Harris, R. C.,  
558 and Takahashi, T. (2007) Deficiency of endothelial nitric-oxide synthase confers  
559 susceptibility to diabetic nephropathy in nephropathy-resistant inbred mice. *Am J Pathol*  
560 **170**, 1473-1484
- 561 17. Zhang, M. Z., Wang, S., Yang, S., Yang, H., Fan, X., Takahashi, T., and Harris, R. C.  
562 (2012) Role of blood pressure and the renin-angiotensin system in development of  
563 diabetic nephropathy (DN) in eNOS<sup>-/-</sup> db/db mice. *Am J Physiol Renal Physiol* **302**,  
564 F433-438
- 565 18. Brosius, F. C., 3rd, Alpers, C. E., Bottinger, E. P., Breyer, M. D., Coffman, T. M.,  
566 Gurley, S. B., Harris, R. C., Kakoki, M., Kretzler, M., Leiter, E. H., Levi, M., McIndoe,  
567 R. A., Sharma, K., Smithies, O., Susztak, K., Takahashi, N., Takahashi, T., and Animal  
568 Models of Diabetic Complications, C. (2009) Mouse models of diabetic nephropathy.  
569 *Journal of the American Society of Nephrology : JASN* **20**, 2503-2512

- 570 19. O'Brien, P. D., Hur, J., Hayes, J. M., Backus, C., Sakowski, S. A., and Feldman, E. L.  
571 (2014) BTBR ob/ob mice as a novel diabetic neuropathy model: Neurological  
572 characterization and gene expression analyses. *Neurobiol Dis* **73C**, 348-355
- 573 20. Zhang, H., Nair, V., Saha, J., Atkins, K. B., Hodgins, J. B., Saunders, T. L., Myers, M.  
574 G., Jr., Werner, T., Kretzler, M., and Brosius, F. C. (2017) Podocyte-specific JAK2  
575 overexpression worsens diabetic kidney disease in mice. *Kidney Int*
- 576 21. Zhang, H., Saha, J., Byun, J., Schin, M., Lorenz, M., Kennedy, R. T., Kretzler, M.,  
577 Feldman, E. L., Pennathur, S., and Brosius, F. C., 3rd. (2008) Rosiglitazone reduces  
578 renal and plasma markers of oxidative injury and reverses urinary metabolite  
579 abnormalities in the amelioration of diabetic nephropathy. *Am J Physiol Renal Physiol*  
580 **295**, F1071-1081
- 581 22. Laboratory, B. Determination of Podocyte Number and Density in Rodent Glomeruli. In  
582 *Animal Models of Diabetic Complications Consortium*
- 583 23. Biessels, G. J., van der Heide, L. P., Kamal, A., Bleyers, R. L., and Gispen, W. H. (2002)  
584 Ageing and diabetes: implications for brain function. *Eur J Pharmacol* **441**, 1-14
- 585 24. Zhang, H., Saha, J., Byun, J., Schin, M., Lorenz, M., Kennedy, R. T., Kretzler, M.,  
586 Feldman, E. L., Pennathur, S., and Brosius, F. C. (2008) Rosiglitazone reduces renal  
587 and plasma markers of oxidative injury and reverses urinary metabolite abnormalities in  
588 the amelioration of diabetic nephropathy. *American Journal of Physiology-Renal*  
589 *Physiology* **295**, F1071-F1081
- 590 25. Sanden, S. K., Wiggins, J. E., Goyal, M., Riggs, L. K., and Wiggins, R. C. (2003)  
591 Evaluation of a thick and thin section method for estimation of podocyte number,  
592 glomerular volume, and glomerular volume per podocyte in rat kidney with Wilms'  
593 tumor-1 protein used as a podocyte nuclear marker. *Journal of the American Society of*  
594 *Nephrology* **14**, 2484-2493
- 595 26. Zhang, H., Schin, M., Saha, J., Burke, K., Holzman, L. B., Filipiak, W., Saunders, T.,  
596 Xiang, M., Heilig, C. W., and Brosius, F. C., 3rd. (2010) Podocyte-specific  
597 overexpression of GLUT1 surprisingly reduces mesangial matrix expansion in diabetic  
598 nephropathy in mice. *Am J Physiol Renal Physiol* **299**, F91-98

- 599 27. Oh, S. S., Hayes, J. M., Sims-Robinson, C., Sullivan, K. A., and Feldman, E. L. (2010)  
600 The effects of anesthesia on measures of nerve conduction velocity in male C57Bl6/J  
601 mice. *Neurosci Lett* **483**, 127-131
- 602 28. O'Brien, P. D., Guo, K., Eid, S. A., Rumora, A. E., Hinder, L. M., Hayes, J. M.,  
603 Mendelson, F. E., Hur, J., and Feldman, E. L. (2020) Integrated lipidomic and  
604 transcriptomic analyses identify altered nerve triglycerides in mouse models of  
605 prediabetes and type 2 diabetes. *Dis Model Mech* **13**
- 606 29. Trapnell, C., Roberts, A., Goff, L., Pertea, G., Kim, D., Kelley, D. R., Pimentel, H.,  
607 Salzberg, S. L., Rinn, J. L., and Pachter, L. (2012) Differential gene and transcript  
608 expression analysis of RNA-seq experiments with TopHat and Cufflinks. *Nature*  
609 *protocols* **7**, 562-578
- 610 30. Kramer, A., Green, J., Pollard, J., Jr., and Tugendreich, S. (2014) Causal analysis  
611 approaches in Ingenuity Pathway Analysis. *Bioinformatics* **30**, 523-530
- 612 31. Ashburner, M., Ball, C. A., Blake, J. A., Botstein, D., Butler, H., Cherry, J. M., Davis,  
613 A. P., Dolinski, K., Dwight, S. S., Eppig, J. T., Harris, M. A., Hill, D. P., Issel-Tarver,  
614 L., Kasarskis, A., Lewis, S., Matese, J. C., Richardson, J. E., Ringwald, M., Rubin, G.  
615 M., and Sherlock, G. (2000) Gene ontology: tool for the unification of biology. The  
616 Gene Ontology Consortium. *Nat Genet* **25**, 25-29
- 617 32. Maity, S., Das, F., Kasinath, B. S., Ghosh-Choudhury, N., and Ghosh Choudhury, G.  
618 (2020) TGF $\beta$  acts through PDGFR $\beta$  to activate mTORC1 via the Akt/PRAS40 axis and  
619 causes glomerular mesangial cell hypertrophy and matrix protein expression. *J Biol*  
620 *Chem*
- 621 33. Jiang, G., Hu, C., Tam, C. H., Lau, E. S., Wang, Y., Luk, A. O., Yang, X., Kong, A. P.,  
622 Ho, J. S., Lam, V. K., Lee, H. M., Wang, J., Zhang, R., Tsui, S. K., Ng, M. C., Szeto, C.  
623 C., Jia, W., Fan, X., So, W. Y., Chan, J. C., and Ma, R. C. (2016) Genetic and clinical  
624 variables identify predictors for chronic kidney disease in type 2 diabetes. *Kidney Int*  
625 **89**, 411-420
- 626 34. Shi, Y., Huang, C., Zhao, Y., Cao, Q., Yi, H., Chen, X., and Pollock, C. (2020) RIPK3  
627 blockade attenuates tubulointerstitial fibrosis in a mouse model of diabetic nephropathy.  
628 *Sci Rep* **10**, 10458

- 629 35. Takahashi, T., and Harris, R. C. (2014) Role of endothelial nitric oxide synthase in  
630 diabetic nephropathy: lessons from diabetic eNOS knockout mice. *J Diabetes Res* **2014**,  
631 590541
- 632 36. Hinder, L. M., Murdock, B. J., Park, M., Bender, D. E., O'Brien, P. D., Rumora, A. E.,  
633 Hur, J., and Feldman, E. L. (2018) Transcriptional networks of progressive diabetic  
634 peripheral neuropathy in the db/db mouse model of type 2 diabetes: An inflammatory  
635 story. *Experimental neurology* **305**, 33-43
- 636 37. McGregor, B. A., Eid, S., Rumora, A. E., Murdock, B., Guo, K., de Anda-Jauregui, G.,  
637 Porter, J. E., Feldman, E. L., and Hur, J. (2018) Conserved Transcriptional Signatures in  
638 Human and Murine Diabetic Peripheral Neuropathy. *Sci Rep* **8**, 17678
- 639 38. Vincent, A. M., Hayes, J. M., McLean, L. L., Vivekanandan-Giri, A., Pennathur, S., and  
640 Feldman, E. L. (2009) Dyslipidemia-induced neuropathy in mice: the role of  
641 oxLDL/LOX-1. *Diabetes* **58**, 2376-2385
- 642 39. Hur, J., Sullivan, K. A., Pande, M., Hong, Y., Sima, A. A., Jagadish, H. V., Kretzler,  
643 M., and Feldman, E. L. (2011) The identification of gene expression profiles associated  
644 with progression of human diabetic neuropathy. *Brain : a journal of neurology* **134**,  
645 3222-3235
- 646 40. Manea, S. A., Constantin, A., Manda, G., Sasson, S., and Manea, A. (2015) Regulation  
647 of Nox enzymes expression in vascular pathophysiology: Focusing on transcription  
648 factors and epigenetic mechanisms. *Redox Biol* **5**, 358-366
- 649 41. Hur, J., Dauch, J. R., Hinder, L. M., Hayes, J. M., Backus, C., Pennathur, S., Kretzler,  
650 M., Brosius, F. C., 3rd, and Feldman, E. L. (2015) The Metabolic Syndrome and  
651 Microvascular Complications in a Murine Model of Type 2 Diabetes. *Diabetes* **64**,  
652 3294-3304
- 653 42. Mifsud, S. A., Allen, T. J., Bertram, J. F., Hulthen, U. L., Kelly, D. J., Cooper, M. E.,  
654 Wilkinson-Berka, J. L., and Gilbert, R. E. (2001) Podocyte foot process broadening in  
655 experimental diabetic nephropathy: amelioration with renin-angiotensin blockade.  
656 *Diabetologia* **44**, 878-882
- 657 43. Azushima, K., Gurley, S. B., and Coffman, T. M. (2018) Modelling diabetic  
658 nephropathy in mice. *Nat Rev Nephrol* **14**, 48-56

- 659 44. Hodgin, J. B., Nair, V., Zhang, H., Randolph, A., Harris, R. C., Nelson, R. G., Weil, E.  
660 J., Cavalcoli, J. D., Patel, J. M., Brosius, F. C., 3rd, and Kretzler, M. (2013)  
661 Identification of cross-species shared transcriptional networks of diabetic nephropathy  
662 in human and mouse glomeruli. *Diabetes* **62**, 299-308
- 663 45. Wilson, P. C., Wu, H., Kirita, Y., Uchimura, K., Ledru, N., Rennke, H. G., Welling, P.  
664 A., Waikar, S. S., and Humphreys, B. D. (2019) The single-cell transcriptomic  
665 landscape of early human diabetic nephropathy. *Proc Natl Acad Sci U S A* **116**, 19619-  
666 19625
- 667 46. Shahzad, K., Bock, F., Dong, W., Wang, H., Kopf, S., Kohli, S., Al-Dabet, M. M.,  
668 Ranjan, S., Wolter, J., Wacker, C., Biemann, R., Stoyanov, S., Reymann, K.,  
669 Soderkvist, P., Gross, O., Schwenger, V., Pahernik, S., Nawroth, P. P., Grone, H. J.,  
670 Madhusudhan, T., and Isermann, B. (2015) Nlrp3-inflammasome activation in non-  
671 myeloid-derived cells aggravates diabetic nephropathy. *Kidney Int* **87**, 74-84
- 672 47. Boini, K. M., Xia, M., Abais, J. M., Li, G., Pitzer, A. L., Gehr, T. W., Zhang, Y., and  
673 Li, P. L. (2014) Activation of inflammasomes in podocyte injury of mice on the high fat  
674 diet: Effects of ASC gene deletion and silencing. *Biochim Biophys Acta* **1843**, 836-845
- 675 48. Sun, L., and Kanwar, Y. S. (2015) Relevance of TNF-alpha in the context of other  
676 inflammatory cytokines in the progression of diabetic nephropathy. *Kidney Int* **88**, 662-  
677 665
- 678 49. Elmarakby, A. A., and Sullivan, J. C. (2012) Relationship between oxidative stress and  
679 inflammatory cytokines in diabetic nephropathy. *Cardiovasc Ther* **30**, 49-59
- 680 50. Gurley, S. B., Ghosh, S., Johnson, S. A., Azushima, K., Sakban, R. B., George, S. E.,  
681 Maeda, M., Meyer, T. W., and Coffman, T. M. (2018) Inflammation and Immunity  
682 Pathways Regulate Genetic Susceptibility to Diabetic Nephropathy. *Diabetes* **67**, 2096-  
683 2106
- 684 51. Zheng, X., Soroush, F., Long, J., Hall, E. T., Adishesha, P. K., Bhattacharya, S., Kiani,  
685 M. F., and Bhalla, V. (2017) Murine glomerular transcriptome links endothelial cell-  
686 specific molecule-1 deficiency with susceptibility to diabetic nephropathy. *PLoS One*  
687 **12**, e0185250
- 688 52. Zhang, Z., Zhang, Y., Ning, G., Deb, D. K., Kong, J., and Li, Y. C. (2008) Combination  
689 therapy with AT1 blocker and vitamin D analog markedly ameliorates diabetic

- 690 nephropathy: blockade of compensatory renin increase. *Proceedings of the National*  
691 *Academy of Sciences of the United States of America* **105**, 15896-15901
- 692 53. Zain, M., and Awan, F. R. (2014) Renin Angiotensin Aldosterone System (RAAS): its  
693 biology and drug targets for treating diabetic nephropathy. *Pak J Pharm Sci* **27**, 1379-  
694 1391
- 695 54. Gupta, G., Dahiya, R., Singh, Y., Mishra, A., Verma, A., Gothwal, S. K., Aljabali, A. A.  
696 A., Dureja, H., Prasher, P., Negi, P., Kapoor, D. N., Goyal, R., Tambuwala, M. M.,  
697 Chellappan, D. K., and Dua, K. (2020) Monotherapy of RAAS blockers and  
698 mobilization of aldosterone: A mechanistic perspective study in kidney disease. *Chem*  
699 *Biol Interact* **317**, 108975
- 700 55. Roscioni, S. S., Heerspink, H. J., and de Zeeuw, D. (2014) The effect of RAAS  
701 blockade on the progression of diabetic nephropathy. *Nat Rev Nephrol* **10**, 77-87
- 702 56. Perlman, A. S., Chevalier, J. M., Wilkinson, P., Liu, H., Parker, T., Levine, D. M.,  
703 Sloan, B. J., Gong, A., Sherman, R., and Farrell, F. X. (2015) Serum Inflammatory and  
704 Immune Mediators Are Elevated in Early Stage Diabetic Nephropathy. *Ann Clin Lab*  
705 *Sci* **45**, 256-263
- 706 57. Matoba, K., Takeda, Y., Nagai, Y., Kawanami, D., Utsunomiya, K., and Nishimura, R.  
707 (2019) Unraveling the Role of Inflammation in the Pathogenesis of Diabetic Kidney  
708 Disease. *Int J Mol Sci* **20**
- 709 58. Barutta, F., Bruno, G., Grimaldi, S., and Gruden, G. (2015) Inflammation in diabetic  
710 nephropathy: moving toward clinical biomarkers and targets for treatment. *Endocrine*  
711 **48**, 730-742
- 712 59. Eid, S., Sas, K. M., Abcouwer, S. F., Feldman, E. L., Gardner, T. W., Pennathur, S., and  
713 Fort, P. E. (2019) New insights into the mechanisms of diabetic complications: role of  
714 lipids and lipid metabolism. *Diabetologia* **62**, 1539-1549
- 715 60. Sas, K. M., Lin, J., Rajendiran, T. M., Soni, T., Nair, V., Hinder, L. M., Jagadish, H. V.,  
716 Gardner, T. W., Abcouwer, S. F., Brosius, F. C., 3rd, Feldman, E. L., Kretzler, M.,  
717 Michailidis, G., and Pennathur, S. (2018) Shared and distinct lipid-lipid interactions in  
718 plasma and affected tissues in a diabetic mouse model. *J Lipid Res* **59**, 173-183



- 719 61. Herman-Edelstein, M., Scherzer, P., Tobar, A., Levi, M., and Gafter, U. (2014) Altered  
720 renal lipid metabolism and renal lipid accumulation in human diabetic nephropathy. *J*  
721 *Lipid Res* **55**, 561-572
- 722 62. Liu, Y., Huang, H., Gao, R., and Liu, Y. (2020) Dynamic Phenotypes and Molecular  
723 Mechanisms to Understand the Pathogenesis of Diabetic Nephropathy in Two Widely  
724 Used Animal Models of Type 2 Diabetes Mellitus. *Front Cell Dev Biol* **8**, 172
- 725 63. Chittka, D., Banas, B., Lennartz, L., Putz, F. J., Eidenschink, K., Beck, S., Stempf, T.,  
726 Moehle, C., Reichelt-Wurm, S., and Banas, M. C. (2018) Long-term expression of  
727 glomerular genes in diabetic nephropathy. *Nephrol Dial Transplant* **33**, 1533-1544
- 728 64. Callaghan, B. C., Gao, L., Li, Y., Zhou, X., Reynolds, E., Banerjee, M., Pop-Busui, R.,  
729 Feldman, E. L., and Ji, L. (2018) Diabetes and obesity are the main metabolic drivers of  
730 peripheral neuropathy. *Ann Clin Transl Neurol* **5**, 397-405
- 731 65. Guo, K., Eid, S. A., Elzinga, S. E., Pacut, C., Feldman, E. L., and Hur, J. (2020)  
732 Genome-wide profiling of DNA methylation and gene expression identifies candidate  
733 genes for human diabetic neuropathy. *Clin Epigenetics* **12**, 123
- 734 66. Kallenborn-Gerhardt, W., Hohmann, S. W., Syhr, K. M., Schroder, K., Sisignano, M.,  
735 Weigert, A., Lorenz, J. E., Lu, R., Brune, B., Brandes, R. P., Geisslinger, G., and  
736 Schmidtko, A. (2014) Nox2-dependent signaling between macrophages and sensory  
737 neurons contributes to neuropathic pain hypersensitivity. *Pain* **155**, 2161-2170
- 738 67. Kim, D., You, B., Jo, E. K., Han, S. K., Simon, M. I., and Lee, S. J. (2010) NADPH  
739 oxidase 2-derived reactive oxygen species in spinal cord microglia contribute to  
740 peripheral nerve injury-induced neuropathic pain. *Proc Natl Acad Sci U S A* **107**,  
741 14851-14856
- 742 68. Williams, A. S., Trefts, E., Lantier, L., Grueter, C. A., Bracy, D. P., James, F. D., Pozzi,  
743 A., Zent, R., and Wasserman, D. H. (2017) Integrin-Linked Kinase Is Necessary for the  
744 Development of Diet-Induced Hepatic Insulin Resistance. *Diabetes* **66**, 325-334
- 745 69. del Nogal, M., Luengo, A., Olmos, G., Lasa, M., Rodriguez-Puyol, D., Rodriguez-  
746 Puyol, M., and Calleros, L. (2012) Balance between apoptosis or survival induced by  
747 changes in extracellular-matrix composition in human mesangial cells: a key role for  
748 ILK-NFkappaB pathway. *Apoptosis* **17**, 1261-1274

- 749 70. Shonesy, B. C., Thiruchelvam, K., Parameshwaran, K., Rahman, E. A.,  
750 Karuppagounder, S. S., Huggins, K. W., Pinkert, C. A., Amin, R., Dhanasekaran, M.,  
751 and Suppiramaniam, V. (2012) Central insulin resistance and synaptic dysfunction in  
752 intracerebroventricular-streptozotocin injected rodents. *Neurobiol Aging* **33**, 430 e435-  
753 418
- 754 71. Jurga, A. M., Piotrowska, A., Makuch, W., Przewlocka, B., and Mika, J. (2017)  
755 Blockade of P2X4 Receptors Inhibits Neuropathic Pain-Related Behavior by Preventing  
756 MMP-9 Activation and, Consequently, Pronociceptive Interleukin Release in a Rat  
757 Model. *Front Pharmacol* **8**, 48
- 758 72. Kawasaki, Y., Xu, Z. Z., Wang, X., Park, J. Y., Zhuang, Z. Y., Tan, P. H., Gao, Y. J.,  
759 Roy, K., Corfas, G., Lo, E. H., and Ji, R. R. (2008) Distinct roles of matrix  
760 metalloproteases in the early- and late-phase development of neuropathic pain. *Nat Med*  
761 **14**, 331-336
- 762 73. Bhatt, L. K., and Veeranjanyulu, A. (2010) Minocycline with aspirin: a therapeutic  
763 approach in the treatment of diabetic neuropathy. *Neurol Sci* **31**, 705-716
- 764 74. Ali, S., Driscoll, H. E., Newton, V. L., and Gardiner, N. J. (2014) Matrix  
765 metalloproteinase-2 is downregulated in sciatic nerve by streptozotocin induced  
766 diabetes and/or treatment with minocycline: Implications for nerve regeneration. *Exp*  
767 *Neurol* **261**, 654-665
- 768 75. Li, S. Y., Huang, P. H., Yang, A. H., Tarng, D. C., Yang, W. C., Lin, C. C., Chen, J.  
769 W., Schmid-Schonbein, G., and Lin, S. J. (2014) Matrix metalloproteinase-9 deficiency  
770 attenuates diabetic nephropathy by modulation of podocyte functions and  
771 dedifferentiation. *Kidney Int* **86**, 358-369

## Figure Legends

Figure 1. Diabetic kidney disease (DKD) phenotype for the 8 experimental groups to demonstrate both the separate and combined effects of diabetes status (*db/db*) and *eNOS* deletion. Urine volume (panel A), albuminuria (panel B), and mesangial expansion as quantified by mesangial index (panel C) increased by diabetes alone, but not by *eNOS* deletion alone. Albuminuria, mesangial index, and the percentage of totally sclerosed glomeruli increased in *db/db eNOS*<sup>-/-</sup> compared to *db/db eNOS*<sup>+/+</sup> animals (panels B-D). There were only occasional sclerosed glomeruli in the nondiabetic groups (up to a maximum of 2.2% in the *eNOS*<sup>-/-</sup> nondiabetic mice; not shown) so these were not included in the analysis. RAS inhibitor treatment significantly ameliorated both albuminuria and mesangial expansion in the *db/db eNOS*<sup>-/-</sup> animals. \**p* < 0.05, \*\*\**p* < 0.001. T, indicates RAS inhibitor treatment.

Figure 2. Diabetic peripheral neuropathy (DPN) phenotype for the 8 experimental groups to demonstrate the effects of diabetes and *eNOS* deletion. Sural (Panel A) and sciatic (Panel B) nerve conduction velocities (NCVs) decreased in *db/db* animals, but were not influenced by either *eNOS* deletion or RAS inhibitor treatment. Similarly, latency to withdrawal of hind paw (Panel C) was modestly increased in diabetes but was not clearly affected by *eNOS* deletion \**p* < 0.05, \*\*\**p* < 0.001. T, indicates RAS inhibitor treatment.

Figure 3. Hierarchical clustering of the 8 experimental groups based on genome-wide changes in glomerular gene expression (Panel A). This clustering placed the mice in an order that generally corresponded to DKD severity based on functional and pathologic features (Panel B). The same color code used in panel B to differentiate the different experimental groups is later used for Fig. 4, panel B. One unexpected aspect of the hierarchical clustering is that RAS inhibitor treatment was associated with glomerular gene expression changes that were generally correlated with increasing, not decreasing, DKD severity. The hierarchical clustering suggested that diabetes (*db/db*) has a major effect on gene expression, whereas *eNOS* deletion exerted minor effect in the same direction. T, indicates RAS inhibitor treatment.

Figure 4. Self-organizing map (SOM) (panel A) for glomerular gene expression changes in the 8 experimental groups to demonstrate the response to diabetes (*db/db*), *eNOS* knockout, and RAS inhibition. All gene expression patterns were projected onto a 7 x 7 module (panel A). Each module (hexagon) contains

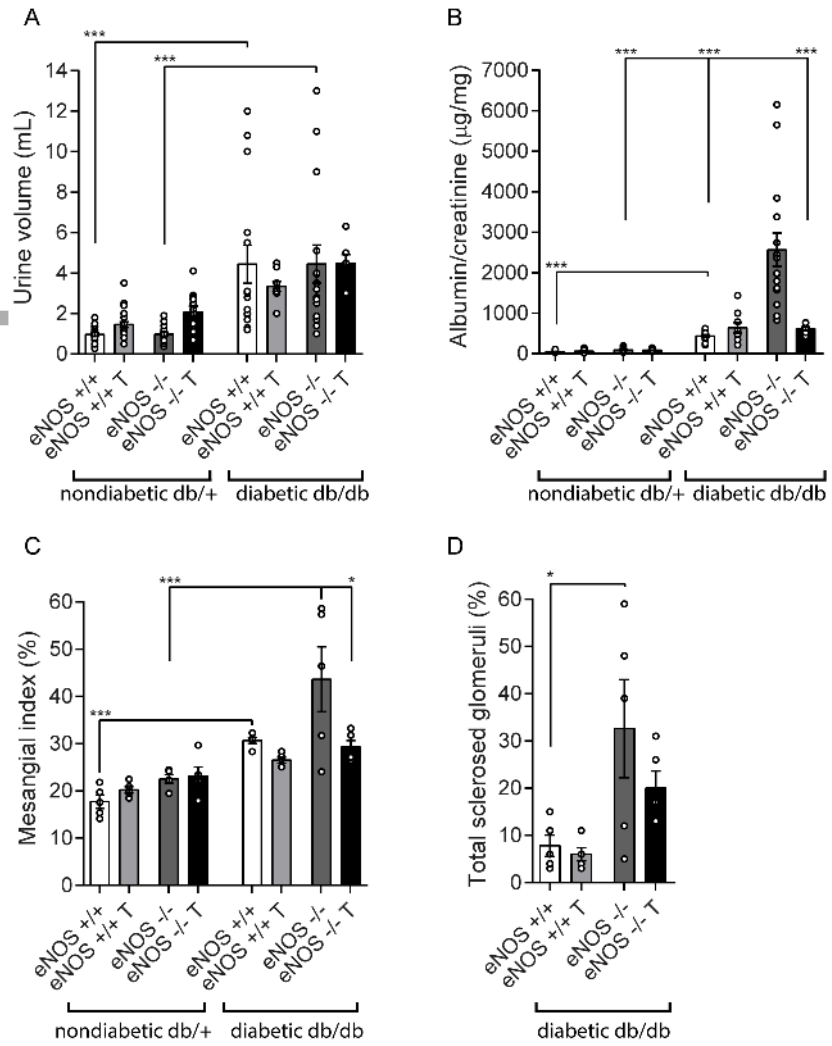
genes with similar expression patterns across the groups (panel B). Hierarchical cluster analysis of the SOM (see Fig. 3) orders the groups as shown in panel B and serves as its legend. Gene expression patterns for each of the 49 modules are depicted in panel B, where numbers correspond to the hexagons from panel A, with 1,1 representing the upper left hexagon and 7,7 the lower right hexagon. Colors and outlines of gene expression changes in each module correspond to the legend in Fig. 3, panel B. Units with similar gene expression patterns that show ordered increases or decreases across the 8 groups are indicated in insets C and D. A total of 1403 genes were identified whose gene expression pattern correlated positively with more normal, undiseased phenotypes (inset C), while expression of 1354 genes correlated positively with more abnormal, diseased phenotypes (inset D). These gene groups were used for further analysis (see Fig. 5).

Figure 5. The correlation between albuminuria and mesangial index was determined with the genes for the most extreme and informative modules (1,1 and 7,7 on the SOM upper left and lower right corners, respectively [Fig. 4]). The top panel shows the aggregate gene expression values in modules 1,1 and 7,7 for each animal. Correlation between the aggregate gene expression values (from modules 1,1 or 7,7) and albuminuria (middle panel) and mesangial index (bottom panel). For all panels, the green points represent the aggregate gene expression for the most “normal” animal group (*db/+ eNOS +/+* treated), while the red points represent the gene expression for the most “diseased” animal group (*db/db eNOS -/-* untreated). T, indicates RAS inhibitor treatment.

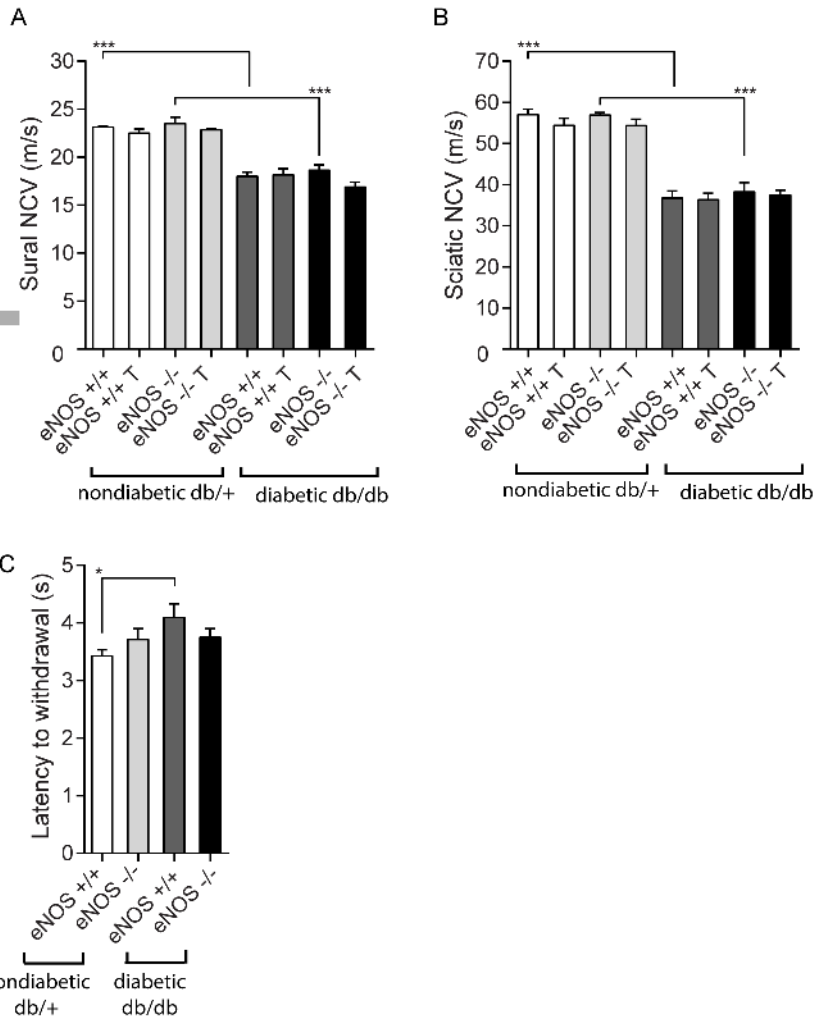
Figure 6. Transcriptomics data analysis of dorsal root ganglia (DRG) tissue collected from *db/db eNOS -/-* animals with or without RAS blockade indicated that treatment enhanced expression of several genes involved in DPN pathogenesis. The top 20 differentially expressed genes (DEGs) in DRG from *db/db eNOS -/-* treated vs. untreated mice are listed in panel A. Functional enrichment analysis of DEGs was performed by IPA, and the 20 most significantly enriched canonical pathways are illustrated in dot plots (panel B). Rich factor refers to the proportion of DEGs belonging to a specific IPA term. Node size (gene number) refers to the number of DEGs within each term, while node color indicates significance level ( $-\log_{10} p$ -value). FC, fold-change; FDR, false discovery rate.

Treatment	db/+ eNOS+/+		db/+ eNOS-/-		db/db eNOS+/+		db/db eNOS-/-	
	none	lisinopril/ losartan	none	lisinopril/ losartan	none	lisinopril/ losartan	none	lisinopril/ losartan
BW (g)	32.0 ± 0.4 (23)	30.4 ± 0.4 (22)	30.6 ± 0.5 (19)	29.2 ± 0.3 (12)	51.8 ± 1.8 (12) *	52.3 ± 4.9 (9) *	46.2 ± 2.1 (15) *	41.1 ± 2.1 (7) *
FBG (mmol/L)	10.4 ± 0.4 (23)	9.5 ± 0.4 (22)	11.0 ± 0.7 (19)	9.1 ± 0.6 (12)	38.7 ± 1.1 (15) *	37.1 ± 1.6 (9) *	35.7 ± 2.7 (15) *	41.1 ± 0.6 (7) *
GHb (%)	5.3 ± 0.1 (22)	5.8 ± 0.2 (21)	5.7 ± 0.2 (16)	5.9 ± 0.2 (12)	12.9 ± 0.4 (12) *	14.2 ± 0.3 (9) *	13.3 ± 0.2 (14) *	14.4 ± 0.6 (7)
SBP (mmHg)	95.1 ± 3.0 (6)	86.5 ± 3.4 (11)	110.8 ± 6.9 (6)	78.1 ± 5.2 (4)	89.7 ± 4.9 (5)	94.6 ± 3.6 (6)	110.5 ± 14.8 (4)	102.7 ± 10.2 (4)
DBP (mmHg)	71.1 ± 2.6 (6)	59.6 ± 2.2 (11)	85.6 ± 5.9 (6)	60.6 ± 4.8 (4)	69.0 ± 1.3 (5)	75.3 ± 2.8 (6)	84.8 ± 10.5 (4)	82.3 ± 11.6 (4)
Trig (mmol/L)	0.91 ± 0.17 (10)	1.10 ± 0.1 (4)	0.8 ± 0.11 (9)	1.2 ± 0.13 (8)	1.22 ± 0.23 (7)	1.4 ± 0.21 (8)	1.73 ± 0.39 (8) †	1.11 ± 0.22 (7)
Chol (mmol/L)	2.02 ± 0.1 (10)	1.81 ± 0.15 (4)	2.24 ± 0.12 (9)	2.43 ± 0.13 (8)	2.56 ± 0.19 (7)	3.04 ± 0.28 (8)	3.66 ± 0.52 (8) †	3.26 ± 0.27 (7)
HDL (mmol/L)	1.52 ± 0.08 (10)	1.21 ± 0.08 (4)	1.74 ± 0.12 (9)	1.72 ± 0.13 (8)	1.78 ± 0.13 (7)	1.91 ± 0.22 (8)	2.11 ± 0.36 (8)	2.2 ± 0.21 (7)
LKW (g)	0.23 ± 0.01 (21)	0.22 ± 0.01 (21)	0.20 ± 0.01 (18)	0.20 ± 0.01 (12)	0.28 ± 0.02 (12) *	0.26 ± 0.01 (9)	0.22 ± 0.02 (15) †	0.24 ± 0.01 (7)

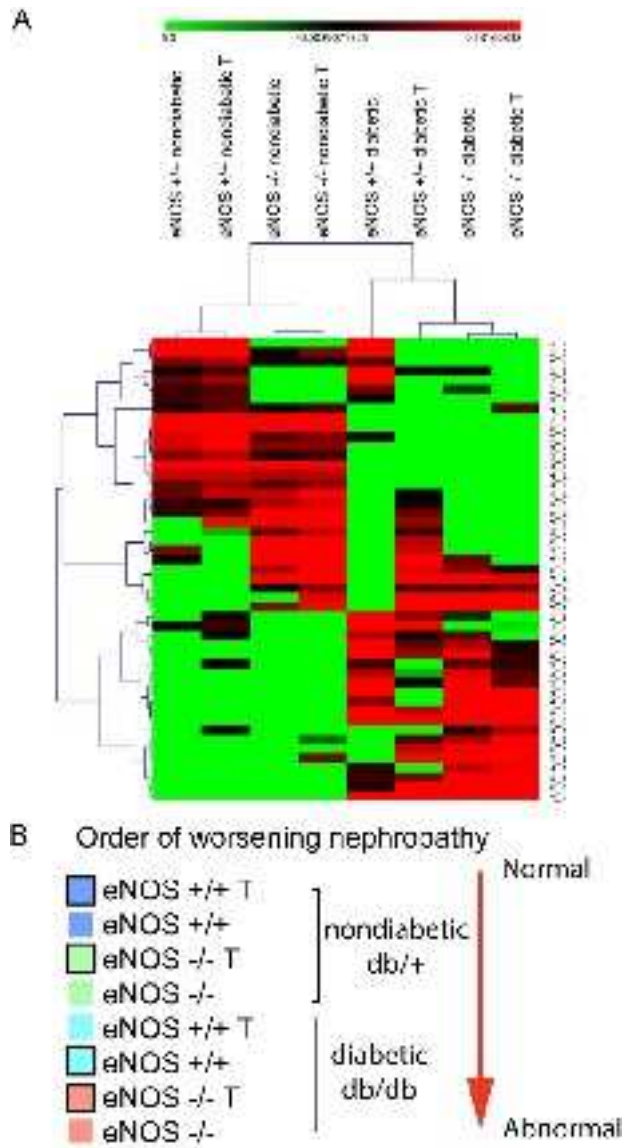
Table 1. Physiological data. All values are from the study endpoint. BW, body weight; FBG, fasting blood glucose; GHb, glycated hemoglobin; SBP, systolic blood pressure; DBP, diastolic blood pressure, Trig, triglycerides; Chol, total cholesterol; HDL, high-density lipoprotein cholesterol; LKW, left kidney weight. Data are presented as mean ± standard error of the mean, with total number of animals in parentheses. \* vs. Control; † vs. db/+ eNOS -/- mice. p < 0.05.



fsb2\_21467\_f1.tif

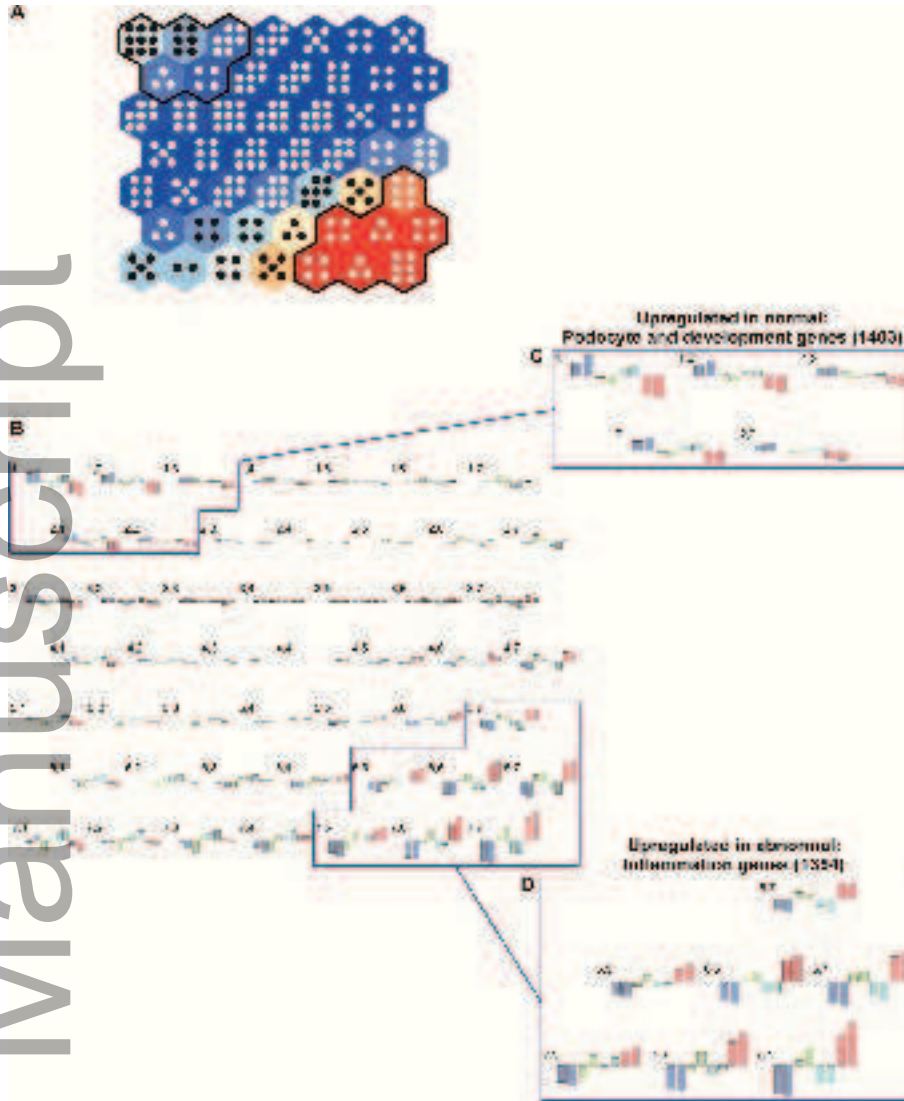


fsb2\_21467\_f2.tif

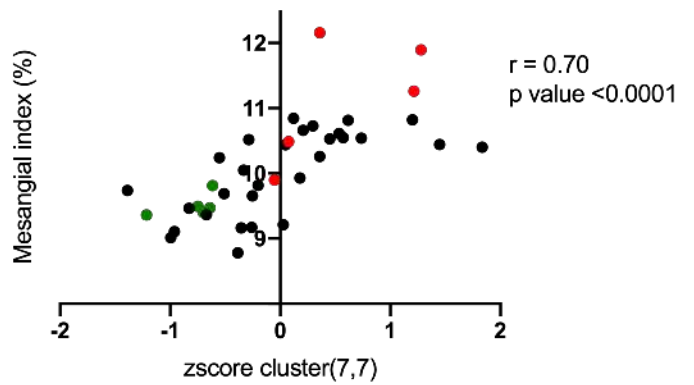
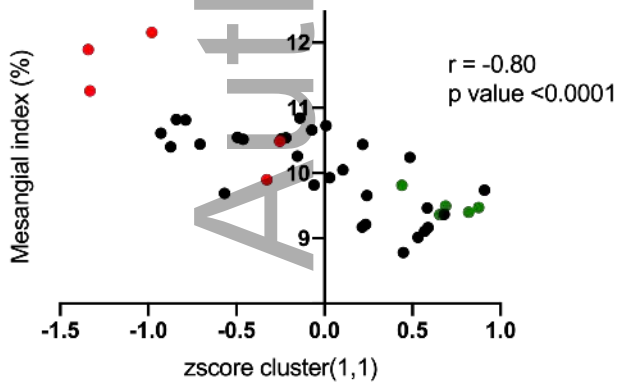
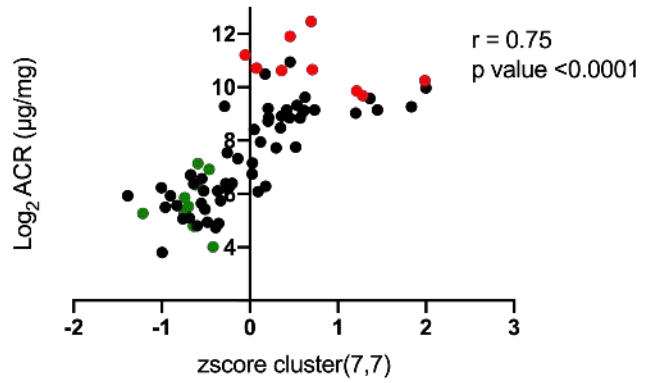
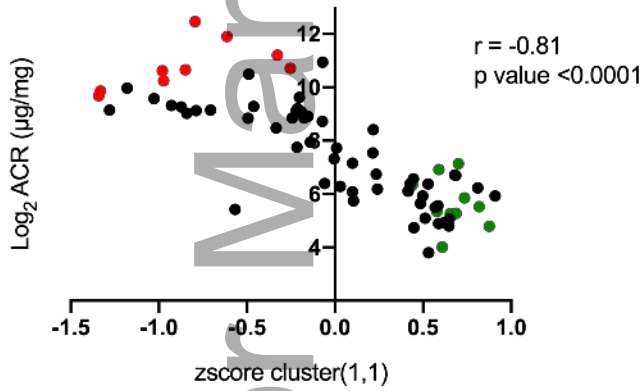
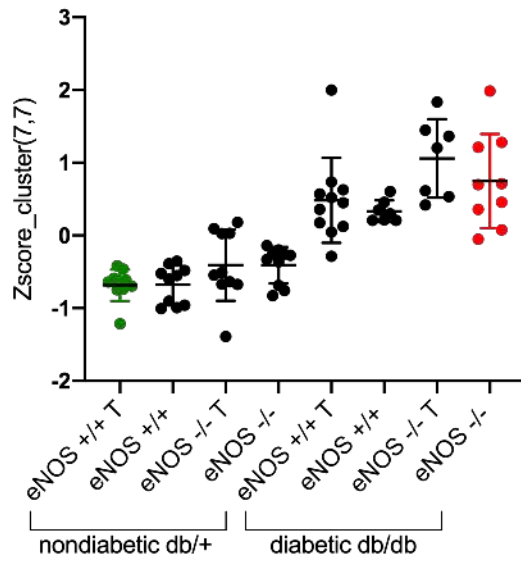
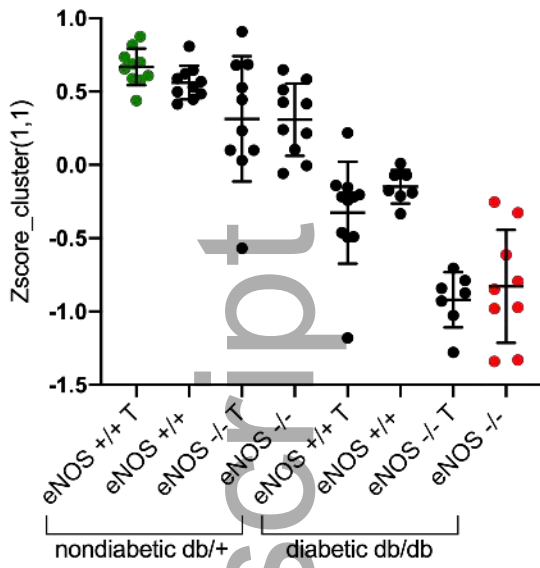


fsb2\_21467\_f3.tif





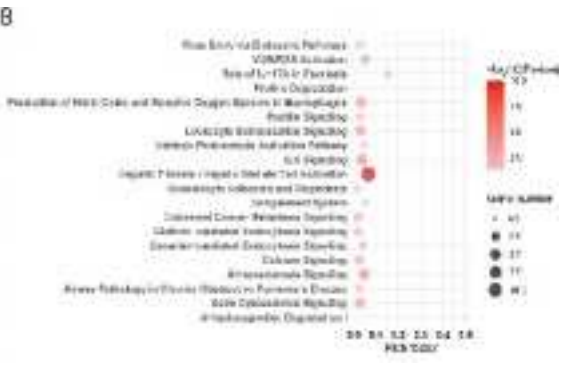
fsb2\_21467\_f4.tif



fsb2\_21467\_f5.tif

**A**

Gene ID	Symbol	Description	FC	Padj
1241	Agg1	Protein tyrosine phosphatase, cytosolic	1.12	0.01
1414	Agg2	Aggrecan	0.76	0.01
1742	Agg3	Aggrecan-like 1	0.65	0.01
1801	Agg4	Aggrecan-like 2	0.73	0.01
1802	Agg5	Aggrecan-like 3	0.71	0.01
1803	Agg6	Aggrecan-like 4	0.78	0.01
1804	Agg7	Aggrecan-like 5	0.68	0.01
1805	Agg8	Aggrecan-like 6	0.71	0.01
1806	Agg9	Aggrecan-like 7	0.71	0.01
1807	Agg10	Aggrecan-like 8	0.71	0.01
1808	Agg11	Aggrecan-like 9	0.71	0.01
1809	Agg12	Aggrecan-like 10	0.71	0.01
1810	Agg13	Aggrecan-like 11	0.71	0.01
1811	Agg14	Aggrecan-like 12	0.71	0.01
1812	Agg15	Aggrecan-like 13	0.71	0.01
1813	Agg16	Aggrecan-like 14	0.71	0.01
1814	Agg17	Aggrecan-like 15	0.71	0.01
1815	Agg18	Aggrecan-like 16	0.71	0.01
1816	Agg19	Aggrecan-like 17	0.71	0.01
1817	Agg20	Aggrecan-like 18	0.71	0.01
1818	Agg21	Aggrecan-like 19	0.71	0.01
1819	Agg22	Aggrecan-like 20	0.71	0.01
1820	Agg23	Aggrecan-like 21	0.71	0.01
1821	Agg24	Aggrecan-like 22	0.71	0.01
1822	Agg25	Aggrecan-like 23	0.71	0.01
1823	Agg26	Aggrecan-like 24	0.71	0.01
1824	Agg27	Aggrecan-like 25	0.71	0.01
1825	Agg28	Aggrecan-like 26	0.71	0.01
1826	Agg29	Aggrecan-like 27	0.71	0.01
1827	Agg30	Aggrecan-like 28	0.71	0.01
1828	Agg31	Aggrecan-like 29	0.71	0.01
1829	Agg32	Aggrecan-like 30	0.71	0.01
1830	Agg33	Aggrecan-like 31	0.71	0.01
1831	Agg34	Aggrecan-like 32	0.71	0.01
1832	Agg35	Aggrecan-like 33	0.71	0.01
1833	Agg36	Aggrecan-like 34	0.71	0.01
1834	Agg37	Aggrecan-like 35	0.71	0.01
1835	Agg38	Aggrecan-like 36	0.71	0.01
1836	Agg39	Aggrecan-like 37	0.71	0.01
1837	Agg40	Aggrecan-like 38	0.71	0.01
1838	Agg41	Aggrecan-like 39	0.71	0.01
1839	Agg42	Aggrecan-like 40	0.71	0.01
1840	Agg43	Aggrecan-like 41	0.71	0.01
1841	Agg44	Aggrecan-like 42	0.71	0.01
1842	Agg45	Aggrecan-like 43	0.71	0.01
1843	Agg46	Aggrecan-like 44	0.71	0.01
1844	Agg47	Aggrecan-like 45	0.71	0.01
1845	Agg48	Aggrecan-like 46	0.71	0.01
1846	Agg49	Aggrecan-like 47	0.71	0.01
1847	Agg50	Aggrecan-like 48	0.71	0.01
1848	Agg51	Aggrecan-like 49	0.71	0.01
1849	Agg52	Aggrecan-like 50	0.71	0.01
1850	Agg53	Aggrecan-like 51	0.71	0.01
1851	Agg54	Aggrecan-like 52	0.71	0.01
1852	Agg55	Aggrecan-like 53	0.71	0.01
1853	Agg56	Aggrecan-like 54	0.71	0.01
1854	Agg57	Aggrecan-like 55	0.71	0.01
1855	Agg58	Aggrecan-like 56	0.71	0.01
1856	Agg59	Aggrecan-like 57	0.71	0.01
1857	Agg60	Aggrecan-like 58	0.71	0.01
1858	Agg61	Aggrecan-like 59	0.71	0.01
1859	Agg62	Aggrecan-like 60	0.71	0.01
1860	Agg63	Aggrecan-like 61	0.71	0.01
1861	Agg64	Aggrecan-like 62	0.71	0.01
1862	Agg65	Aggrecan-like 63	0.71	0.01
1863	Agg66	Aggrecan-like 64	0.71	0.01
1864	Agg67	Aggrecan-like 65	0.71	0.01
1865	Agg68	Aggrecan-like 66	0.71	0.01
1866	Agg69	Aggrecan-like 67	0.71	0.01
1867	Agg70	Aggrecan-like 68	0.71	0.01
1868	Agg71	Aggrecan-like 69	0.71	0.01
1869	Agg72	Aggrecan-like 70	0.71	0.01
1870	Agg73	Aggrecan-like 71	0.71	0.01
1871	Agg74	Aggrecan-like 72	0.71	0.01
1872	Agg75	Aggrecan-like 73	0.71	0.01
1873	Agg76	Aggrecan-like 74	0.71	0.01
1874	Agg77	Aggrecan-like 75	0.71	0.01
1875	Agg78	Aggrecan-like 76	0.71	0.01
1876	Agg79	Aggrecan-like 77	0.71	0.01
1877	Agg80	Aggrecan-like 78	0.71	0.01
1878	Agg81	Aggrecan-like 79	0.71	0.01
1879	Agg82	Aggrecan-like 80	0.71	0.01
1880	Agg83	Aggrecan-like 81	0.71	0.01
1881	Agg84	Aggrecan-like 82	0.71	0.01
1882	Agg85	Aggrecan-like 83	0.71	0.01
1883	Agg86	Aggrecan-like 84	0.71	0.01
1884	Agg87	Aggrecan-like 85	0.71	0.01
1885	Agg88	Aggrecan-like 86	0.71	0.01
1886	Agg89	Aggrecan-like 87	0.71	0.01
1887	Agg90	Aggrecan-like 88	0.71	0.01
1888	Agg91	Aggrecan-like 89	0.71	0.01
1889	Agg92	Aggrecan-like 90	0.71	0.01
1890	Agg93	Aggrecan-like 91	0.71	0.01
1891	Agg94	Aggrecan-like 92	0.71	0.01
1892	Agg95	Aggrecan-like 93	0.71	0.01
1893	Agg96	Aggrecan-like 94	0.71	0.01
1894	Agg97	Aggrecan-like 95	0.71	0.01
1895	Agg98	Aggrecan-like 96	0.71	0.01
1896	Agg99	Aggrecan-like 97	0.71	0.01
1897	Agg100	Aggrecan-like 98	0.71	0.01
1898	Agg101	Aggrecan-like 99	0.71	0.01
1899	Agg102	Aggrecan-like 100	0.71	0.01



fsb2\_21467\_f6.tif

Author Manuscript